

Monitoring cell membrane recycling dynamics of proteins using whole-cell fluorescence recovery after photobleaching of pH-sensitive genetic tags

Piotr Michaluk^{1,2}, Dmitri A Rusakov¹

¹ UCL Queen Square Institute of Neurology, University College London, London, United Kingdom;

² BRAINCITY, Laboratory of Neurobiology, Nencki Institute of Experimental Biology PAS, Warsaw, Poland;

Correspondence should be addressed to D.A.R. (d.rusakov@ucl.ac.uk) or P.M. (p.michaluk@nencki.edu.pl)

EDITORIAL SUMMARY The cell membrane turnover kinetics of the main glial glutamate transporter GLT1 are quantified by fusing it to a pH-sensitive fluorescent protein and performing measurements using whole-cell fluorescence recovery after photobleaching.

PROPOSED TWEET #NewNProt for measuring membrane turnover kinetics of proteins tagged with pH-sensitive fluorescence tags by whole cell FRAP.

PROPOSED TEASER Measuring membrane dynamics with pH-sensitive tags

Related links

Key reference using this protocol

Michaluk, P. et al. *Elife* 10, 64714 (2021): <https://doi.org/10.7554/eLife.64714>

Abstract

Population behaviour of signalling molecules on the cell surface is key to their adaptive function. Live imaging of proteins tagged with fluorescent molecules has been an essential tool in understanding this behaviour. Typically, genetic or chemical tags are used to target molecules present throughout the cell whereas antibody-based tags label the externally exposed molecular domains only. Both approaches could potentially overlook the intricate process of in-out membrane recycling in which target molecules appear or disappear on the cell surface. This limitation is overcome by using a pH-sensitive fluorescent tag, such as Super-Ecliptic pHluorin (SEP), because its emission depends on whether it resides inside or outside the cell. Here, we focus on the main glial glutamate transporter GLT1 and describe a genetic design that equips GLT1 molecules with SEP without interfering with the transporter's main function. Expressing GLT1-SEP in astroglia in cultures or in hippocampal slices enables monitoring the real-time dynamics of the cell-surface and cytosolic fractions of the transporter in living cells. Whole-cell fluorescence recovery after photobleaching (FRAP) and quantitative image-kinetic analysis of the resulting lapse-time images enables assessing the rate of GLT1-SEP recycling on the cell surface, a fundamental trafficking parameter unattainable previously. The present protocol takes 15-20 days to set up cell preparations, and 2-3 days to carry out live cell experiments and data analyses. The protocol can be adapted to study different membrane molecules of interest, particularly those proteins whose lifetime on the cell surface is critical to their adaptive function.

Introduction

The present protocol describes an experimental technique aimed to quantify cell membrane turnover of a protein by using FRAP imaging of its pH-sensitive fluorescent tag¹. Rapid exchange of physiological messages among mammalian cells relies on various signalling molecules expressed on the cell surface. The way such molecules group, migrate, and are recycled in cell membranes has long been considered essential in determining their cellular function. Over the past decades, our understanding of these processes has been revolutionised by the emergence of molecular tagging techniques that use fluorescent proteins or nanoparticles^{2,3}. The arrival of fluorescent fusion tags has prompted the development of imaging methods that reveal population dynamics of the target molecules in living cells with quantitative precision. These methods range from photobleaching and photoactivation^{4,5,6} to single-particle tracking techniques that resolve movements of individual tagged molecules^{7,8} using stochastic reconstruction of light point-source positions⁹. The latter concept has driven rapid progress in monitoring nanoscale topography and trafficking dynamics for various receptor proteins over relatively long time spans^{10,11,12,13}.

While these techniques provide researchers with a capacity to monitor and analyse molecular movements in living cells, detecting cell-membrane insertion and removal of the target molecules remains a non-trivial task. In the case of exogenously applied fluorescent tags, such as antibody-conjugated quantum dots^{8,14} only molecules that are currently exposed to the external medium will be labelled. These tagged molecules may or may not undergo their native recycling process whereas non-tagged molecules could continuously arrive at the cell surface after the labelling has been completed. In the case of fluorescently stable genetic tags^{15,16,17,18,19}, reliable detection of in-out membrane cycling is often beyond the resolution limit of existing imaging methods.

An important breakthrough came with the development of pHluorins, the pH-sensitive mutants of the green fluorescent protein, obtained through structure-directed combinatorial mutagenesis²⁰. One protein variant, superecliptic-pHluorin (SEP), has been engineered to have $pK_a \sim 7.1$, that is to fluoresce when exposed to the extracellular medium ($pH \sim 7.4$) while remaining dark inside the cells, especially within intracellular organelles ($pH < 6$)²¹. Genetic fusion of SEP with synaptic vesicle proteins has enabled direct monitoring of neurotransmitter release^{21,22,23}, but it is the pHluorin tagging of glutamate receptor 2 that has been used inventively to reveal membrane recycling (internalisation) of the receptor's extrasynaptic fraction^{24,25}. The latter approach has paved the way for taking advantage of SEP tagging in assessing protein dynamics and recycling in cell membranes.

Development of the protocol

The excitatory neurotransmitter glutamate is essential for the functioning of central neural circuits. The present protocol focuses on the main glial glutamate transporter, GLT1 is thought to account for the bulk of glutamate uptake in the brain^{26,27}. GLT1 is expressed at high densities in astrocytic membranes²⁸, providing rapid (sub-millisecond scale) neurotransmitter buffering upon synaptic discharges²⁹ followed by slower (tens of milliseconds) translocation into the astrocyte cytoplasm³⁰. Despite the powerful buffering capacities of GLT1, intense

excitatory activity can prompt extrasynaptic glutamate escape, thus potentially involving glutamate receptor activation at neighbouring synapses^{31, 32, 33, 34}. In this context, decreased GLT1 levels, hence reduced glutamate uptake, have long been associated with the development of neurological conditions such as stroke or addiction^{35, 36, 37}. Thus, understanding the membrane dynamics of GLT1 could provide key insights into its adaptive role in regulating brain excitatory signalling. Recent studies employed antibody-conjugated fluorescent quantum dots to characterise quantitatively GLT1 mobility on astrocyte surfaces, under varied physiological scenarios^{38, 39}. While providing important details pertaining to lateral diffusion of GLT1, the externally applied quantum-dot labelling offers little information on membrane insertion and internalisation of the target protein. This prompted us to turn to genetic GLT1 tagging with SEP (Fig. 1a) and measure the kinetic exchange between its membrane and intracellular fractions¹ (Fig. 1b). Thus, SEP-tagged GLT1 (GLT1-SEP) provided us with a biologically relevant example of the general method aimed at a better understanding of membrane protein turnover kinetics.

Once SEP tagging had been implemented, we checked if the tagged protein would fully retain its key functionalities. This was achieved in separate control experiments, by expressing GLT1-SEP in human embryonic kidney (HEK) cells and probing its glutamate transport function using the fast-exchange ligand application protocol described previously⁴⁰. Having thus confirmed the functional integrity of GLT1-SEP, we designed and implemented two stages of the imaging protocol to test GLT1-SEP's membrane recycling in cultured astroglia. In the first stage, one control test was to acidify the extracellular medium to pH 5.5 by applying a 10 second pipette puff of **NH₄Cl-extracellular solution buffered to pH 5.5**, which should reversibly suppress GLT1-SEP fluorescence, thus revealing the surface occurrence of GLT1-SEP and any background fluorescence signal¹ (Fig. 1c). Alternatively, we equilibrated reversibly the pH across the cell membrane by applying NH₄Cl to the bath medium (10 second puff), which made the intracellular GLT1-SEP fraction fluoresce (Fig. 2c; see '*Revealing surface fraction using pH manipulation*'). Analysing these data revealed the surface fraction of GLT1-SEP, also giving the ratio of kinetic constants that characterise its membrane in-out recycling. In the second approach, we developed a whole-cell FRAP imaging protocol (Fig. 1d; '*Whole-cell FRAP: Experiment*') and the kinetic analysis of the resulting lapse-time imaging (Fig. 2; '*Whole-cell FRAP: image analysis*'). Implementing this protocol reveals the rates of membrane insertion and removal for GLT1-SEP, which was unattainable previously. The surface-sensitive SEP tagging protocol was also used to understand the role of the C-terminus in regulating recycling of GLT1 in astroglial membranes¹.

Applications of the method

The present protocol introduces a whole-cell FRAP imaging design and a 'kinetic' image analysis, which rely on genetic tagging and could be adapted to a wide range of proteins in cellular neuroscience and cell biology applications. Technical requirements for the protocol's adaption should be feasible in common experimental settings that involve preparations of cell cultures or thin tissue slices, a laser-scanning microscope system with a photobleaching regime, and molecular biology facilities suitable for genetic manipulations.

In our case, a construct of GLUT1 in fusion with SEP was prepared using standard methodology, taking advantage of the QuikChange II Site-Directed Mutagenesis Kit. While the long-established use of pHluorin tags should facilitate their practical application, a similar approach could be used to tag the protein of interest with red-shifted, pH-sensitive fluorescent proteins, such as pHuji⁴¹ or the recently developed pHmScarlet⁴². The latter approaches could provide chromatic separation (green versus red) for simultaneous imaging of two target surface molecules. We transfected astroglia with the SEP-tagged construct in dissociated primary hippocampal culture using a lipid-based method (Lipofectamine 3000, Thermo Fisher Scientific), but standard viral vector transduction or electroporation methods would also be suitable. In the present protocol, we use a pressurised patch pipette to apply 50 mM NH₄Cl extracellular solution for ~10 s to assess the membrane fraction of the SEP-tagged protein of interest. While this method ensures rapid local application, brief bath application of NH₄Cl would be appropriate for setups that are not equipped with a micromanipulator. In that case, keeping NH₄Cl application time to a minimum⁴³ can be achieved by optimising perfusion settings, such as the flow rate and the total required culture medium volume. A complementary control experiment could involve a reduction of extracellular pH to reveal residual intracellular fluorescence¹.

Whilst we used a two-photon excitation imaging setup with dual scanhead (one for imaging and one for bleaching), most single-scanhead one-photon excitation microscopes are equipped with equally suitable scanning-photobleaching modes that are enabled through their control software. Since the FRAP technique has a long history in estimating diffusion coefficients and protein dynamics^{4, 5, 44}, many commercial imaging systems have built-in capabilities to reproduce the present FRAP protocol. In our hands, the best results were obtained using a 'Tornado' mode for bleaching, where a circular bleaching region is scanned in a spiral fashion starting from the centre^{45, 46}. This regime effectively employs a linescan with a spiral trajectory that in many cases covers the region of interest (ROI) faster compared to the traditional frame (multi-line) scanning in which every line could take as much time as a single spiral scan. The latter feature could be of particular importance when performing FRAP in a large area, which requires significant pixel dwell time while avoiding a distinct linear gradient of photobleaching characteristic for frame (line-by-line) scanning. Microscopes equipped with resonant scanners should also be able to provide a comparable efficiency of the FRAP protocol, by running fast (up to 1-2 kHz) repetitive frame scans over the entire cell until the required level of photobleaching is achieved. Thus, the present protocol could be adapted to the signalling molecule of interest in various experimental settings, particularly for those proteins whose lifetime on the cell surface is critical to their adaptive function.

Comparison with other methods

Classically, the internalised fraction of the molecule of interest can be detected, for example, using a radiolabelled ligand, or after permeabilization with a secondary marker that is different from the one used for the protein's membrane fraction. Such methods have clear limitations as they estimate the recycling kinetics from a single time-point, per individual preparation, and thus are prone to significant errors, particularly in case of high turnover rates. Below we briefly compare the present protocol with other established methods.

Stop-point turnover methods

One method aiming to measure the relative membrane-bound and intracellular fractions of a protein of interest involves biotin labelling and immuno-quantitation of cell-surface proteins^{47, 48, 49}. In this method, two groups of cells are compared, a control sample under inhibited protein trafficking (e.g., at low temperature), and a test sample under permissive conditions (physiological temperature) in which biotinylated surface proteins are internalised. Following a brief internalisation period, surface biotin is cleaved, and an immunoblot is run to detect the internalised fraction in the test group as all membrane surface proteins will be initially biotinylated. While this method has an advantage of working with native, albeit biotinylated, proteins, the procedure is sensitive to the variable outcome of chemical reactions⁴⁸, and is unlikely to suit faster (seconds range) protein turnover rates. Moreover, biotinylation of surface proteins can be problematic in mix-type cultures such as neuronal cultures which are a mixture of different cell types. Biotinylation will not discriminate cell types which might express the same membrane proteins but have different regulation mechanisms.

Similar to the biotin labelling method is an “antibody feeding assay” in which the protein of interest is labelled on the cell surface with a specific antibody^{50, 51}. The unbound antibodies are washed out and cells are incubated at 37°C, to enable endocytosis of the protein for a given length of time, in a time-course experiment. Once the cells are fixed, the permeabilised and internalized fraction of the molecule of interest can be detected with a secondary antibody. Different versions of this method enable studying surface expression, internalisation, and even recycling⁵². One critical limitation of the antibody-based methods is that they often block protein functions such as ligand binding⁵³. For many proteins, there are also no commercially-available antibodies that would target extracellular parts of the protein in conditions of live cell imaging. This leaves one with the choice to either develop an antibody or to introduce a specific tag that can be detected by an antibody. The former solution is time consuming and risks interfering with protein function whereas the latter loses the advantage of studying the native protein.

Another method employs the membrane protein ts-O45-G⁵⁴, which accumulates in the endoplasmic reticulum at 39.5 °C, but is transported to the plasma membrane at 32 °C, and is detected by a fluorescent tag or an antibody⁵⁵. This elegant variation of the 'stop-point turnover' method, however, can only be applied to some selected proteins and its precision lessens with faster time scales of protein turnover. Interpretation of such experiments becomes virtually impossible in models similar to primary dissociated hippocampal culture, which represent a mix of neurons, astrocytes and other glial cells.

An alternative stop-point method focuses on the membrane insertion, rather than internalisation, of the protein of interest, and is based on the specific thrombin (extracellular protease) cleavage site, as well as on antibody feeding⁵⁶. It was originally developed for Protease Activated Receptor 1 which is one of the thrombin receptors⁵⁷. To adapt the method to other proteins, the thrombin cleavage site has to be introduced to the protein of interest using molecular biology methods. It is usually preceded by a specific tag which can be detected by an antibody, for example FLAG⁵⁸. Once cells are incubated with thrombin, the tag is removed from the membrane population of the protein, allowing this population to be distinguished from

the proteins which were inserted into the membrane after the thrombin has been removed from the extracellular solution.

In general, these methods have an overarching limitation: they cannot provide monitoring and assessment of molecular membrane turnover in real time, instead relying on an estimate of recycling kinetics from stop-point data after cell fixation.

Super-resolution microscopy

Relatively direct observation of membrane protein dynamics could be achieved using total reflection fluorescence microscopy, in which fluorescence of the tag is collected from within a nanoscopic submembrane layer⁵⁹. However, this approach normally requires the cell membrane of interest to adhere to a flat glass surface, which narrows the application to specific cell preparations. Another super-resolution method, stimulated emission depletion (STED) microscopy also permits, in principle, optical separation of nanoscopic membrane and sub-membrane domains: combined with stop-start conditions for exocytosis, it can provide excellent readout of protein clustering⁶⁰. However, its optical resolution (>15 nm) may require the exact positioning of the cell membrane to be perpendicular to the plane of view, to distinguish reliably between fluorescence sources located at the membrane surface as opposed to within the adjacent intracellular sub-membrane layer.

Fluorescence Recovery after Photoconversion

An elegant method to gauge accurately the exocytosis rate employs corrected Fluorescence Recovery after Photoconversion, in which exocytosis-dependent and independent trafficking events are measured simultaneously⁶¹. First, the protein under study is tagged with Dendra2, a green-to-red photoconvertible fluorescent protein. Next, Dendra2 in the plasma membrane, localised in the microscope field of view, is photoconverted thus turning red. Finally, both the recovery of the green signal (originally intracellular) and the changes in the photoconverted red signal (originally membrane-bound) are measured⁶¹. Again, while providing real-time readout of the apparent protein turnover, the accuracy of this approach depends on the ability of the imaging system to isolate membrane-only ROIs, preferably on the nanoscale.

Traditional FRAP methods

Classical FRAP experiments rely on bleaching a small region on the cell surface. In such cases, recovery of fluorescence occurs mainly due to fast in-membrane lateral diffusion rather than due to the much slower recycling between membrane and intracellular fractions of the protein. Furthermore, the most popular fluorescent tag for such experiments, GFP, exhibits similar optical properties inside the cell and on its surface. Because photobleaching with the laser occurs within a 0.5-1 μm wide focal layer (characteristic depth of the optical point spread function), the likelihood of bleaching both membrane-bound and internalised GFP-tagged proteins remains relatively high. The latter complicates interpretation of the FRAP results.

In summary, although membrane protein recycling has been extensively studied using various techniques, the majority rely either on 'endocytosis stop-start' experiments based on membrane protein labelling, on having monocultures rather than mixed-cell cultures (to avoid misattribution of microscopic cell compartments), or on highly specific physical arrangements

also involving optical resolution beyond the diffraction limit of light. The present protocol establishes the membrane turnover rate of a protein by analysing whole-cell FRAP dynamics of its pH-sensitive tag, be it SEP or another pH-sensitive protein^{41, 42}, from real-time cell imaging data. Clearly, scientific quests based on the present protocol would benefit from integration with established single-molecule tracking methods^{7, 8}, and in particular those relevant to GLT1^{1, 38, 39}.

Experimental design

The present protocol requires preparation and transfection of a primary neuronal, glial or mixed culture with a DNA construct of a membrane protein in fusion with SEP (or another pH-sensitive protein of choice). If the corresponding construct is not available, it has to be prepared. The critical step is to properly choose the site for SEP introduction. Firstly, one has to make sure that SEP is exposed to the extracellular space once on the cell surface (Fig. 1a). Secondly, care should be taken to avoid any part of the protein which is crucial for protein function such as the sites that may affect ligand binding, channel opening, glycosylation, disulphide bonds, signal peptides, etc. Additionally, it is worth considering to introduce a linker between SEP and the protein of interest depending on the possible functionality of the site of insertion. One can find a good discussion of linker properties in a paper of Chen and colleagues⁶².

Primary neuronal cultures and other preparations

Sprague-Dawley rat pups (postnatal day P0) were used to prepare dissociated hippocampal cultures used in the Procedure below, in accord with the modified protocols that were described in detail previously^{63, 64}. In brief, after 3 hr post plating, the plating medium was exchanged for the maintenance medium (Neurobasal A without phenol red, 2% B 27 supplement, 1% penicillin-streptomycin, 0.5 mM glutaMAX, 25 mM β -mercaptoethanol; Thermo Fisher Scientific) and cells were kept at 37°C, under a humidified 5% CO₂. A similar approach is used to plate and maintain primary neurons from other cortical brain regions⁶². Whilst the present protocol focuses on primary cell cultures, it can be adapted to brain slices prepared in accord with the standard procedures for either acute or organotypic preparations⁶⁵, provided that several key conditions are met as follows. Firstly, the laser scanning area should cover at least 90% of the visible cell territory. Secondly, the expression of a pH-sensitive fluorescent tag in individual cells should be seen against a non-fluorescent background of the surrounding tissue. Finally, scanning regimes of the microscope should include a 3D-scan option that would allow uninterrupted laser scanning over the x , y , and z axes covering >90% of the 3D cell territory. Other organised-tissue slices can also be examined with the present method, provided that similar conditions are met, and there are no principal obstacles in adapting the present approach to in vivo experiments.

Transfection

Cells are transfected with the plasmids using the method of choice, for example calcium-phosphate ⁶⁶. Here, we have used Lipofectamine 3000 (Thermo Fisher Scientific) at 7–10 days in vitro, as described in steps 23–28 of the procedure. The lipofectamine–DNA complexes are prepared in accord with the standard manufacturer instructions (https://assets.thermofisher.com/TFS-Assets/LSG/manuals/lipofectamine3000_protocol.pdf) and incubated with plated primary neurons for ~1 hr (in the incubator) in freshly prepared medium. After the incubation, the conditioned maintenance medium is returned to the cells. Experiments are normally performed at 14–19 days in vitro when the neuronal culture is mature and the protein tag fluorescence is clearly seen (Fig. 3a). Depending on the biological question asked, cells can be transfected much earlier, even on the day of plating, for example by electroporation with Amaxa® Nucleofector®. This would apply especially for studies on developing neurons and often expression of a transgene, can be observed as early as the day following transfection.

Assessing key functions of the tagged protein

This part of experimental design describes how to test the functional integrity of the protein under study. The specific tests to assess GLT1-SEP function have been described in the original paper ¹. The specific controls for functional integrity should be adapted to the protein of interest. Once the DNA construct has been created one should perform control experiments to confirm that SEP introduction has no adverse effects on the main function of the protein under study. This can be done by expressing the fusion protein in a model system and comparing its function with that of the original (wild-type) protein expressed in a similar system. In the case of GLT1, the main protein function is glutamate transport whereas other target proteins could be tested for ligand-induced channel opening or other signalling actions. We have checked the functionality of GLT1-SEP by expressing it in HEK293 cells (subclone Lenti-X 293T, TaKaRa). We recorded the GLT1-SEP and GLT1 expressing cells in whole-cell mode and briefly applied a 1 s long 1 mM glutamate solution pulse using a pressurised rapid-solution-exchange system, as detailed previously ⁴⁰. The transporter current, which is proportional to the transported amount of glutamate, was measured using a standard patch clamp technique in HEK293 cells ⁶⁷ transfected with either wild-type or SEP-fused protein. Comparing the current-voltage curves between the two groups confirmed unperturbed transporter function of the SEP-tagged protein ¹.

Revealing surface fraction using pH manipulation: example of control experiment

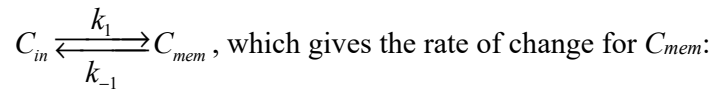
The purpose of this control experiment is to obtain an independent estimate of the surface fraction of a tagged protein. The outcome should confirm the surface fraction estimate obtained with the whole-cell FRAP, and correct any errors that might in some cases arise from the (low) residual fluorescence emitted by the intracellular tag (see *Limitations*). . . . A coverslip with transfected cells (astrocytes in mixed hippocampal culture) is placed in an open recording chamber, under a microscope objective, equipped with a heated perfusion system maintaining a close-to-physiological temperature. A pressurised pipette (linked to a micropump) filled with either pH 5.5-adjusted bath medium or 50 mM NH₄Cl (pH 7.4) in extracellular solution is

mounted on a standard micromanipulator for electrophysiological recordings (e.g., Scientifica PatchStar, Luigs and Neumann LN Mini25, or other micromanipulators). A fluorescence microscope (e.g., Olympus BX51WI) is tuned to image in the green emission channel, and focused on the transfected cell under study (Fig. 3a). In these baseline conditions fluorescence imaging reports the membrane fraction of GLT1-SEP which fluoresces owing to the higher pH of the extracellular medium, plus any non-specific background fluorescence. First, to verify that the observed fluorescence comes from membrane-expressed SEP-tagged protein, brief (10-20 s) puffs of pH5.5-adjusted extracellular solution are applied, as detailed earlier¹. Acidification of the extracellular environment must reversibly dampen all SEP fluorescence. At this stage, the emission channel reports signal background alone (autofluorescence, etc. which has to be subtracted from informative images during subsequent analyses). Next, similar puffs of extracellular solution containing 50 mM NH₄Cl directed at the imaged cell are applied. This should equilibrate the pH across the cell membrane thus resulting in fluorescence of the intracellular SEP tag in addition to the surface-exposed SEP (Fig. 3b, top row). Here, the emission reports the total level of the tagged protein (plus background signal). To control the extent of the puff, the pipette may also contain a bright biologically neutral tracer, such as Alexa 633 (Fig. 3b, middle row). In this test, relating the fluorescence intensity in baseline conditions to that during the NH₄Cl puff (with background subtracted) indicates the membrane fraction of GLT1-SEP, termed R .

We note that extracellular pH manipulation techniques should be applied with caution, such as using as brief applications of pH-altering altered media as possible, to avoid irreversible perturbation of intracellular pH^{24,25}, which might also be triggered by cell physiological responses (such as receptor actions) to external stimuli⁶⁸.

Revealing surface fraction using pH manipulation: analyses

This experiment, by providing the ratio R between the membrane fraction and the total protein content of GLT1-SEP, or C_{mem} / C_{tot} , sheds light on the kinetics of their exchange. Denoting the rates of GLT1-SEP membrane insertion and removal (endocytosis) as, respectively, k_1 and k_2 , we have a simple kinetic reaction for the protein turnover:



$$\frac{\partial C_{mem}}{\partial t} = k_1 C_{in} - k_{-1} C_{mem}, \text{ which in steady-state (no } C_{mem} \text{ changes) becomes}$$

$$k_1 C_{in} = k_{-1} C_{mem}.$$

Because the total protein content C_{tot} remains constant on the timescale of interest (minutes), we can express C_{in} as

$$C_{in} = C_{tot} - C_{mem}.$$

Substituting thus C_{in} , we obtain the experimentally measured ratio R :

$$R = \frac{C_{mem}}{C_{tot}} = \frac{k_1}{k_1 + k_{-1}}, \text{ which gives us a simple relationship between } k_1 \text{ and } k_{-1}:$$

$$k_{-1} = \left(\frac{1}{R} - 1 \right) k_1 = \beta k_1$$

Whole-cell FRAP: experiment

The whole-cell FRAP method is primarily designed for cultured cells that have in large part a 2D structure (spread flatly over the coverslip), which is characteristic for the majority of primary neuronal cultures. However, modern microscopes with rapid 3D scanning should be able to execute the whole-cell FRAP approach for cells in tissue with complex 3D morphology, including astrocytes that exhibit a high surface-to-volume ratio throughout⁶⁹. The experiment described here requires either a two-photon excitation microscope (we have used Olympus FV1000 system under Olympus XLPlan N25 water immersion objective, NA 1.05; or Femtonics Femto-2D with a similar objective), or another laser scanning confocal microscope, with the capacity of photobleaching-regime scanning over up to a 100 μm wide ROI. Most GFP-based indicators have two two-photon absorption peaks, around 910-930 nm and around 690-720 nm, with the shorter band being more efficient for the fluorophore transition from the ground to a stable non-emitting state, i.e. photobleaching⁷⁰. Our experimental setup was equipped with a dual scanhead and two tuneable fs lasers: this enabled us to optimise the regime of simultaneous imaging and bleaching using the two corresponding excitation spectrum bands.

During the experiment, a live cell preparation is placed under the objective and the microscope is focused on the cell of interest expressing the tagged protein (Fig. 3d). We have used the photobleaching regime involving a spiral ('Tornado') line-scan mode, which enables rapid single-line scanning (up to 2 kHz) over a large area of interest^{1,45,46}. Thus, a circular ROI is selected for photobleaching (ROI-PB, red dashed circle in Fig. 1d diagram; experimental example in Fig. 3d) to cover a large portion (up to 80-90%) of the visible cell morphology. During experimental trials, one begins with field-of-view frame time-series imaging, at low laser power. At a selected time (after 10-20 imaging frames), a brief photobleaching scan within the ROI-PB is applied until the fluorescent signal over ROI-PB is reduced, whereupon time-series imaging at low laser power continues until ROI-PB fluorescence is recovered to a steady-state (not necessarily the original) level (Fig. 3d).

We note that photobleaching is largely an irreversible optical process, and in most cases it only affects molecules that would normally fluoresce, i.e. fluorophore molecules that are prompted to transit from the ground state to the excited state then to a stable non-emitting state. In the cases when the pH-sensitive fluorescent tag shows some residual intracellular fluorescence, the photobleaching sequence should bleach such excited molecules irreversibly. The remaining intact intracellular tagged molecules will still provide unbiased FRAP readout when transported to the cell surface. The potential error in estimating the membrane / intracellular ratio for the protein of interest in such cases is discussed in the Limitations section.

Whole-cell FRAP: image analysis

Once the time-series frame imaging of the FRAP experiment has been recorded, duly catalogued and saved in an appropriate image format, further image analyses can be done off line. To this end, we have used the freely available image analysis platform Fiji (NIH ImageJ2, <https://imagej.nih.gov/>), but other standard imaging platforms equipped with the functions described here should also be suitable, for example Olympus FLUOVIEW, or Molecular Devices MetaMorph.

It is possible that the photobleached area shows incomplete photobleaching, at least in some regions, with relatively heterogeneous fluorescence (Fig. 3d). Incomplete photobleaching may increase noise in the data but it does not affect the outcome of the FRAP analysis (based on the underlying reaction kinetics) because it affects neither the kinetics of protein membrane turnover per se nor the proportion of immobile molecules that show no recovery. In other words, the same reaction kinetic equations (see below) will apply to the entire population of tagged molecules or to a proportion of it. The only potential residual effect of incomplete high-intensity photobleaching is an increased contribution of basal photobleaching (i.e. that during normal, low-intensity imaging), but this can be addressed directly by removing the basal photobleaching trend beforehand, as explained in the next section.

Because photobleaching occurred over a large area with the same laser intensity, the net lateral diffusion flow of intact tagged molecules within the bleached area should be close to zero (ignoring residual influx at the boundary). Thus, selecting multiple small ROIs randomly inside the area should, in theory, cancel out residual effects of membrane diffusion influx or outflux arising from local homogeneities in bleaching efficacy.

To minimise further any such effects, in each recorded time-series (image stack), the investigator selects one or more smaller ROIs inside ROI-PB, so that each smaller ROI covers relatively homogeneous cell membrane structure, is located away from the ROI-PB boundary and is several microns away from any prominent inhomogeneities in the membrane fluorescence (blue dotted circles, Fig. 1d; experimental example in Fig. 4a). We note that lateral diffusivity of GLT1-SEP is in the range of $0.1 \mu\text{m}^2/\text{s}$ (ref. ¹), giving a characteristic lateral diffusion distance of only 2-3 μm over ~ 20 s (GLT1-SEP turnover rate). Thus, the chosen settings should minimise the influence of lateral diffusion on FRAP kinetics. The small ROIs were also selected outside the cell body area, to avoid its non-flat geometry ¹. Next, in each image time-series (frame stack), the average fluorescence intensity values, separately for every ROI, are recorded and plotted against frame time stamps, across the time of the trial. These plots thus represent the raw data for the kinetic FRAP analysis.

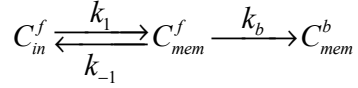
Whole-cell FRAP: estimating protein turnover rates

The typical FRAP recording (Fig. 2a) will include: (a) a segment of either near-constant or slowly decreasing baseline fluorescence, (b) a rapid signal drop to near-zero during the brief laser-scanning photobleaching regime, (c) partial fluorescence recovery due to the appearance of non-bleached tagged protein molecules on the cell surface, and (d) visible slow decay due to residual photobleaching (no decay if the latter is negligible).

The analysis of whole-cell FRAP follows the kinetic reactions representing the process of fluorescence recovery, right after the photobleaching phase, due to the membrane insertion of

unbleached SEP-tagged molecules after a brief period of intense photobleaching (high-intensity laser scanning). An additional reaction represents residual photobleaching, if any, during regular fluorescence-image recording at the required laser power.

C_{mem}^f and C_{in}^f denote the membrane and cytosol fractions, respectively, of non-bleached SEP-tagged molecules; and C_{mem}^b denotes the membrane fraction of the bleached protein. The kinetic reactions between these three components are represented as follows:



where k_1 and k_{-1} are the characteristic rates of membrane insertion and removal, respectively, for the tagged protein, and k_b is the rate of residual (experiment-wise) photobleaching. Replacing $k_{-1} = \beta k_1$ (see *Revealing surface fraction using pH manipulation: analyses* above), the rate of change for C_{in}^f will be given by the linear differential equation:

$$\frac{\partial C_{in}^f}{\partial t} = \beta k_1 C_{mem}^f - k_1 C_{in}^f .$$

the solution for which is

$$C_{in}^f = \beta C_{mem}^f - C_0 e^{-k_1 t} .$$

Similarly, the rate of change for C_{mem}^f is

$$\frac{\partial C_{mem}^f}{\partial t} = k_1 C_{in}^f - \beta k_1 C_{mem}^f - k_b C_{mem}^f .$$

Substituting C_{in}^f as above, we obtain

$$\frac{\partial C_{mem}^f}{\partial t} = -k_1 C_0 e^{-k_1 t} - k_b C_{mem}^f , \text{ with the solution}$$

$$C_{mem}^f = C_1 e^{-k_b t} - \frac{k_1}{k_b - k_1} C_0 e^{-k_1 t} .$$

where C_1 and C_0 are unknown constants. To constrain their values, we consider initial and boundary (limiting) conditions that apply to our experimental setting. Firstly, we note that at the start of FRAP (i.e. immediately after the brief period of full photobleaching, at $t = 0$), it is assumed that $C_{mem}^f = 0$ (this ignores surface molecules that were not photobleached, and whose turnover kinetics can be therefore considered unrelated to FRAP). Substituting this in the above expression gives

$$C_1 = \frac{k_1}{k_b - k_1} C_0 \text{ hence}$$

$$C_{mem}^f = \frac{k_1}{k_b - k_1} C_0 (e^{-k_b t} - e^{-k_1 t}) .$$

Also, under negligible residual fluorescence ($k_b=0$), after full equilibration post hoc ($t \rightarrow \infty$), the remaining unbleached protein assumes the same membrane-cytosol ratio as in baseline conditions:

$$C_{mem}^f(t \rightarrow \infty) = RC_{in}$$

where C_{in} now represents the total unbleached protein after all the initial membrane-bound protein, C_{mem} , was bleached. This gives the normalised fluorescence time course $F(t)$ during FRAP as

$$F(t) = \frac{C_{mem}^f}{C_{mem}} = \frac{C_{in}}{C_{tot}} (e^{-k_b t} - e^{-k_t t}).$$

This expression is used to fit the experimental FRAP data (Fig. 2b).

In practice, the fluorescence time course data collected over individual small ROIs are normalised so that the minimum level (after the high-intensity photobleaching period) is set at zero level and $t = 0$, and the initial fluorescence set at level one (Fig. 4b). Incomplete photobleaching at $t = 0$ does not affect FRAP kinetics and the corresponding kinetic estimates, as explained above, but it may have a residual effect when the basal photobleaching (i.e. during normal, low-intensity imaging) is relatively strong, such as for instance >10% over the characteristic FRAP constant. In such cases, the best way to proceed would be (a) to establish this overall photobleaching trend using baseline imaging, without the FRAP sequence (e.g., by fitting the raw data with a linear or single-exponent decay), and (b) to subtract this trend from the FRAP time course, before carrying out further FRAP analyses. With negligible residual photobleaching ($k_b = 0$; or the photobleaching component subtracted from the original data as explained above, Fig. 4c), this expression has two orthogonal (independent) free parameters, C_{in} and k_t , which allows for a convergent fitting procedure (Fig. 4d). We used non-linear fitting routines in OriginPro (OriginLab, Menu "Analysis/Fitting/Non-linear Curve Fit") but other standard curve fitting tools can be used.

We note that in our case, the immobile fraction, i.e. the intracellular-versus-membrane protein fraction obtained from the FRAP analyses was fully consistent with that obtained using pH manipulation in separate experiments (Fig. 3a-c)¹. This indicated that potential artefacts of photobleaching that might perturb intracellular pH were negligible. In other experimental settings, such control experiments are advisable.

Expertise needed to implement the protocol

No special expertise is needed but experience in live cell imaging, cell culture preparation (particularly primary neuronal culture), and molecular cloning is desirable.

Limitations

The main limitation of the protocol, which is common to all molecular tagging methods, is that it introduces an exogenous protein tag into the molecule of interest, requiring expression of the construct usually under control of an unnatural promoter. This may raise several potential issues. Firstly, care should be taken in choosing the site for SEP introduction, to ensure that the tag is exposed to the extracellular space but also avoid **insertion** sites that may disturb protein function, such as those that may affect ligand binding, channel opening, glycosylation, disulphide bonds, signal peptides, etc. In applying the protocol to GLT1, this issue was dealt with by including a section for comparing the main function of GLT1-SEP, glutamate uptake,

against the glutamate uptake of the native GLT1 molecule¹. In order to account for possible differences in the expression of GLT1 and GLT1-SEP we also measured their expression using immunostaining and Western blot in a control experiment¹. Secondly, introducing SEP – a ~30 kDa globular protein – into the target protein may, in theory, affect protein mobility and trafficking. In this respect, we note that GLT1-SEP in our hands shows similar membrane mobility to that of GLT1 tagged with quantum dots³⁹, and that tagging an extracellular domain is the method that is least likely to interfere with trafficking. In general, it would be important to design control experiments that test the consistency between the trafficking-related properties of tagged and native proteins. Thirdly, expression of the fusion protein in the cells of interest is usually done by transfecting the cells, or transducing them with viral vectors. This entails relatively poor expression control as the protein is effectively overexpressed next to the native protein in the cell, possibly resulting in competition between tagged and native proteins for binding partners or even membrane space. Again, in the GLT1-specific case, super-resolution visualisation (using dSTORM) of GLT1-SEP and native GLT1 confirmed that the surface patterns of either protein in the astroglial membrane were similar¹. The use of cell-type-specific promoters is limited as they lack complicated transcription control and chromatin context and can drive expression in different cell types than intended ('leaky promoters')⁷¹. Tuning the expression of the target construct is highly time consuming since it requires preparing new transgenic cell lines, which is not possible for primary cell cultures like neurons, or knock-in animals (which takes roughly one year). Another possible solution is to knock-down the native protein with shRNA and introduce a modified construct expressing the fusion protein that is resistant to the shRNA. However even this solution is complex and provides no natural expression control in varied experimental conditions: even the genes considered to be expressed constitutively are often regulated in certain conditions⁷².

Another potential limitation relates to the cases when the intracellular protein fraction is much larger than the membrane and intracellular tags emit residual, albeit low-level, fluorescence. In such cases, the FRAP time course will still report the unbiased turnover kinetics because the intense photobleaching stimulus will leave intact the majority of intracellular tagged molecules that will fluoresce once on the cell surface. However, the estimate of the membrane-versus-intracellular fraction ratio (immobile fraction reported by FRAP) could be biased in such circumstances. Instead, this estimation should be carried out using pH manipulation: silencing the surface tag will reveal the residual intracellular fluorescence¹.

The present method can be readily applied to surface-adherent, or flatly spread, cultured cells because fast bleaching of a large cell region is carried out virtually within one focal plane. In such cases, FRAP analyses carried out close to the cell nucleus could be biased because cell dimensions there significantly exceed the focal plane width. However, modern two-photon excitation or confocal microscopes, with fast piezo Z-motor driven 3-D scanning modes, will enable rapid scanning of the entire target cell across the volume, thus allowing for the use of the present protocol in tissue with three-dimensional organisation.

Materials

BIOLOGICAL MATERIALS

- Primary hippocampal culture prepared from P0 rats. The procedure for obtaining the culture is based on the previously published version^{63, 64}, and uses papain rather than trypsin for tissue digestion. It is described in detail in steps 5-22 of the Procedure.

CAUTION: Appropriate national laws and institutional regulatory board guidelines must be followed for animal work. In our studies, the dissociated hippocampal cultures from P0 Sprague-Dawley rats were prepared in full compliance with the national guideline and the European Communities Council Directive of November 1986, and the European Directive 2010/63/EU on the Protection of Animals used for Scientific Purposes.

CRITICAL: There are many protocols for preparing primary cultures from the brain tissue, and where applicable for the biological question other types of cells can be used, including cell lines. Other protocols for culturing primary brain cells will likely require different reagents then listed below.

REAGENTS

- MEM, no glutamine, no phenol red, (Thermo Fisher Scientific, Cat. No. 51200038)
- GlutaMAX™ Supplement, (Thermo Fisher Scientific, Cat. No. 35050061)
- Neurobasal™-A Medium, minus phenol red (Thermo Fisher Scientific, Cat. No. 12349015)

CRITICAL: For culturing cells for live imaging we recommend using media without phenol red as this dye increases auto-fluorescence of the sample.

- B-27™ Supplement (50X), serum free (Thermo Fisher Scientific, Cat. No. 17504044)
- Fetal Bovine Serum, certified, heat inactivated (Thermo Fisher Scientific, Cat. No. 10082147)

CRITICAL: Good quality of the serum is essential for proper attachment and development of the primary cultured cells. We recommend using certified and heat inactivated serum as low quality serum will often result in overabundance of glial cells, particularly microglia and might even cause neuronal death.

- Penicillin-Streptomycin [5,000 U/mL] (ThermoFisher Scientific, Cat. No. 15070063)
- Poly-DL-Lysine (Sigma-Aldrich, cat. no. P9011)
- Laminin (Sigma-Aldrich, cat. no. L2020)
- Trypan Blue Solution, 0.4% (ThermoFisher Scientific, Cat. No. 15250061)
- 0.5 % Phenol Red Solution (Sigma, Cat. No. P0290)
- L-Cysteine hydrochloride monohydrate (Sigma, Cat. No. C7880)
- Lipofectamine™ 3000 Transfection Reagent (Thermo Fisher Scientific, Cat. No. L3000008)
- Alexa Fluor 633 Hydrazide (Thermo Fisher Scientific, Cat. No. A30634)
- QuikChange II XL Site-Directed Mutagenesis Kit (Agilent, Cat. No. 200522)
- NEBuilder® HiFi DNA Assembly Cloning Kit (New England Biolabs, Cat. No. E5520S)
- Papain, Suspension 100 mg (Worthington, Cat. No. LS003126)
- Standard salts and reagents for buffer preparation – HEPES, MES, NaCl, KCl, CaCl₂, MgSO₄, K₂SO₄, Na₂SO₄, MgCl₂, D-glucose, NaOH, HCl (molecular biology grade reagents can be obtained from any supplier)

CAUTION: NaOH and HCl are corrosive. Wear protective gloves and clothing.

EQUIPMENT

Two-photon imaging setup (or other laser scanning microscope suitable for photobleaching). We used an Olympus FV1000 system based on a BX61 WI motorized Olympus upright microscope equipped with Olympus XLPlanN 25× water immersion objective (NA 1.05). Our imaging system is equipped in 2 independent scanning heads (one for imaging and one for uncaging/bleaching) linked to two mode-locked, femtosecond-pulse Ti:Sapphire lasers (MaiTai from SpectraPhysics-Newport and Chameleon from Coherent). This setup helps optimise the regime of simultaneous imaging and bleaching using two two-photon absorption maxima for GFP-based indicators, as explained above in the FRAP section; the wavelengths we used were ~920 nm imaging and ~690 nm for photobleaching^{70, 73}. The imaging setup could however include a single laser, with the appropriate control to enable rapid switching between imaging and bleaching modes. The system should also be equipped with a trigger-box (TTL output or similar) to provide synchronisation between imaging and peripheral equipment that drives electrical recordings or puffing. Tubing system and peristaltic pump are required for the perfusion system.

Motorized micromanipulator (Scientifica; PatchStar Micromanipulator),

Standard patch pipette puller (Sutter Instrument; Model P-1000)

glass capillaries for pulling pipettes (World Precision Instruments; Cat. No. 1B150F-4)

Pneumatic PicoPump (World Precision Instruments, Cat. No. SYS-PV830)

Standard molecular biology equipment (pipettes, PCR machine, agarose gel electrophoresis apparatus, 37°C incubator and shaker, centrifuge)

Micro-dissecting forceps (Merck, Cat. No. F4142),

Jewelers forceps, Dumont No. 5 (Merck, Cat. No. F6521)

Micro-dissecting scissors (Merck, Cat. No. S3146)

Micro spatulas (Merck, Cat. No. Z193216)

Surgical scissors (Fine Science Tools, Cat. No. 14001-18)

Coverslip Mini-Rack (Thermo Fisher Scientific, Cat. No. C14784)

37°C humidified incubator

laminar flow hood

24-well plates

cell counting chamber, Bürker pattern (Merck, cat. No. BR718920-1EA)

13-mm round coverslips (Hecht Assistent, Cat. No. 41001113)

REAGENT SETUP

Borate Buffer (0.1 M, pH 8.5)

Prepare 0.1 M solution of boric acid and 0.1 M solution of sodium tetraborate. Add sodium tetraborate solution to boric acid solution until pH reaches 8.5. Filter sterilize and keep at 4°C for up to 6 months.

Dissociation Medium (DM)

Dissolve 81.8 mM Na₂SO₄, 30 mM K₂SO₄, 5.8 mM MgCl₂, 0.25 mM CaCl₂, 1 mM HEPES pH 7.4, 20 mM glucose, and 0.001% vol/vol Phenol Red in ultrapure water, adjust pH to 7.4 using 1M NaOH and filter sterilize. Keep at 4°C for up to 1 month.

10× KyMg solution

Combine 10 mM Kynurenic acid, 100mM MgCl₂, 0.0025 % vol/vol Phenol Red, 5 mM HEPES, adjust pH to 7.4 and filter sterilize. Store as 5-10 ml aliquots at -20°C for up to 6 months.

Dissociation Medium with Kynureic acid (DM/Ky)

Prepare fresh on the day of use by combining 45 ml of DM and 5 ml of 10x KyMg solution.

Papain Solution

Prepare fresh on the day of use by dissolving 100 units (U) papain suspension and 4.5 mg L-cysteine in 9.8 ml DM/Ky. Mix and keep stirring at 37°C to help dissolve the papain. Adjust pH to 7.4 using 10-20 µl 1M NaOH and filter sterilize. Keep at 4°C. At least 30 minutes before use plate the solution at 37°C.

Plating Medium

Prepare fresh on the day of use by supplementing MEM with 10% vol/vol certified fetal bovine serum (FBS) and 1% vol/vol Penicilin-Streptomycin. Warm up to 37°C and incubate in the incubator for at least 30 minutes before use to adjust the pH. Do not store.

Maintenance Medium

Prepare fresh on the day of use by supplementing Neurobasal-A medium without Phenol Red with 2% vol/vol B-27 supplement, 1% vol/vol Penicillin-Streptomycin, 0.5 mM glutaMAX and 25 µM β-mercaptoethanol. Warm up to 37°C and incubate in the incubator for at least 30 minutes before use to adjust the pH. Do not store.

Extracellular Solution (ES)

Dissolve 125 mM NaCl, 2.5 mM KCl, 30 mM Glucose, 25 mM HEPES, 2 mM CaCl₂ and 1.3 mM MgSO₄ in ultrapure water and adjust the pH to 7.4 using 1M NaOH. Filter sterilize and keep at 4°C for up to a month. The solution can be stored in ≥ 20 ml aliquots and kept at -20°C for up to 6 months.

Extracellular Solution with 50mM NH₄Cl (NH₄Cl-ES)

Dissolve 50 mM NH₄Cl, 75 mM NaCl, 2.5 mM KCl, 30 mM Glucose, 25 mM HEPES, 2 mM CaCl₂ and 1.3 mM MgSO₄ in ultrapure water and adjust the pH to 7.4 using 1M NaOH. Filter sterilize and keep at 4°C for up to a month. The solution can be stored in ≥ 20 ml aliquots and kept at -20°C for up to 6 months.

pH 5.5 Extracellular Solution (pH5.5-ES)

Dissolve 125 mM NaCl, 2.5 mM KCl, 30 mM Glucose, 25 mM MES, 2 mM CaCl₂ and 1.3 mM MgSO₄ in ultrapure water and adjust the pH to 5.5 using 1M NAOH. Filter sterilize and keep at 4°C for up to a month. The solution can be stored in ≥ 20 ml aliquots and kept at -20°C for up to 6 months.

PROCEDURE

Preparing DNA construct of membrane protein fused with SEP TIMING 2 weeks

CRITICAL This protocol describes monitoring GLT1-SEP membrane dynamics using an expression construct where SEP was introduced into the second extracellular loop of GLT1. For preparing DNA constructs of other membrane proteins in fusion with SEP please consider that the introduced SEP should be expressed outside the cell (usually on the N-terminus of the membrane protein or extracellular loop). Try to avoid sites which can affect protein function such as signalling peptide on N-terminus, glycosylation sites, ligand binding sites, proximity to channel pore, etc.

1. Introduce a unique restriction site into the cDNA of the membrane protein of interest cloned into a plasmid. This will enable introducing SEP into a reading frame in the desired position. Using QuikChange II Site-Directed Mutagenesis Kit according to manufacturer's instruction, first perform PCR with appropriately design primers (you can use The QuikChange Primer Design Program <https://www.agilent.com/store/primerDesignProgram.jsp>), then digest the parental methylated plasmid DNA with *DpnI*, transform competent cells and plate them on agar plates containing the appropriate antibiotic for the plasmid vector. For our studies we introduced a single *MluI* site in the second extracellular loop of **rat** GLT1, between two proline residues (P199 and P200).
2. Identify a positive clone by isolating plasmid DNA using a suitable plasmid miniprep kit and screening for the introduced restriction site by restriction digest and gel electrophoresis.
3. Amplify SEP cDNA by PCR with appropriately designed primers and subclone it into the introduced restriction site in the cDNA of the membrane of interest using for example NEBuilder HiFi DNA Assembly Cloning Kit. Transform competent cells and plate them on agar plates containing the appropriate antibiotic for the plasmid vector. In our studies, using PCR, we have also introduced linkers at the N-terminus of SEP (LVPRGSGG) and at the C-terminus of SEP (GGSGSTSGT) to distance the fluorescent molecule from the GLT extracellular loop.
4. Identify positive clones by isolating plasmid DNA using a suitable plasmid miniprep kit and perform restriction digestion analysis. Sequence the resulting plasmid for undesired mutations.

CRITICAL STEP: It is vital to confirm the correct sequence of the resulting DNA construct by Sanger Sequencing. Mutations may affect protein folding, or even introduce stop codons resulting in expression of truncated protein.

5. Purify high quality plasmid for subsequent transfection using one of many available plasmid purification kits. Measure plasmid concentration and it keep at -20°C. Plasmids kept at -20°C are stable for years.

CRITICAL STEP: High quality of plasmid is important as it will affect transfection efficiency and health of the culture after transfection.

PAUSE POINT

Preparing coverslips for cell culture TIMIN: 2 days, 5h hands-on time

CRITICAL This protocol was used to monitor GLT1-SEP in astrocytes in primary hippocampal culture obtained from P0 rats but it can be easily adapted to any adherent culture.

6. At least 2 days before culturing cells, place coverslips in Coverslip Mini-Racks, rinse twice for 10 minutes in distilled water to remove dust and place in a container with freshly prepared 2M NaOH.

CAUTION NaOH is corrosive, wear protective gloves and clothing.

CRITICAL STEP Proper cleaning of coverslips is essential for good cell adherence and maintaining the neuronal culture healthy. At each step of the cleaning procedure care should be taken to keep coverslips separated in racks.

7. Place the container in a sonicating water bath and sonicate for 10 minutes at RT.
8. Rinse coverslips in racks at least 10 times with distilled water over a period of 1 h. After the final rinse, leave racks with coverslips in a container with water.
9. Place the container in a sonicating water bath and sonicate for 10 minutes at RT.
10. Remove racks from water, rinse in absolute ethanol and air-dry under a laminar flow hood. Bake in an oven at 180°C for 2h and cool to room temperature (RT, 18-23°C).
PAUSE POINT Coverslips can be stored in sterile dish at RT for up to a month. However, the longer they are kept, the more contaminants they absorb which negatively affects the coating and adherence of the cells.
11. Two days before culturing cells, place coverslips in 24-well plates and coat with 1 mg/ml poly-DL-Lysine in Borate Buffer (around 40 µl per coverslip). Leave wrapped in an aluminium foil overnight at RT on bench.
12. Remove poly-DL-Lysine, rinse three times with sterile water, 1h each, briefly air-dry coverslips and coat with 10 µg/ml laminin in PBS supplemented with 1 mM CaCl₂ and 0.5 mM MgCl₂. Wrap plates with Parafilm and leave them at 4°C overnight.
13. On the day of culturing cells, aspirate remaining laminin solution and add 0.5 ml Plating Medium to each well.

Preparing mixed hippocampal culture TIMING 2-3 h hands-on time, 1 week growth

14. Kill P0 (postnatal day 0) pups using an approved method of euthanasia, remove brains, place them in ice-cold DM/Ky and isolate hippocampi using dissecting tools.

CAUTION When choosing a method of euthanasia follow the national/local guidelines for work on animals. Our dissociated hippocampal cultures from P0 Sprague-Dawley rats were prepared in full compliance with the national guideline and the European Communities Council Directive of November 1986, and the European Directive 2010/63/EU on the Protection of Animals used for Scientific Purposes.

CRITICAL STEP Removal of the brains and hippocampi isolation should be done quickly and the tissue should be always kept on ice in cold DM/Ky until papain digestion.

15. Rinse hippocampi with ice-cold DM/Ky and incubate in a round-bottom tube in 5 ml of Papain Solution at 37°C for 15 minutes. Gently agitate the tube from time to time.

16. Repeat the incubation in a fresh 5 ml of Papain Solution.
17. Rinse hippocampi three times in 5 ml of DM/Ky and three times in 5 ml of Plating Medium.
18. Triturate the tissue in 1 ml of plating medium until no clumps are visible using a 1 ml pipette tip.
CRITICAL STEP Pipette gently up and down only as many times as necessary. Do not form bubbles.
19. Dilute to 10 ml in MEM pre-warmed to 37°C, centrifuge for 5 minutes at 200 x g, at RT and discard the supernatant.
20. Gently resuspend the cell pellet in 1 ml of Plating Medium per hippocampus.
21. Mix an aliquot of the cell suspension 1:1 with Trypan Blue solution and determine the cell density by counting live cells in a haemocytometer. The yield should be approximately 900,000 – 1,000,000 cells per hippocampus.
22. Plate 75,000 cells per 13-mm round coverslip (from step 12) and put plates in humidified incubator at 37°C.
23. Two – four h after plating, check if most of the cells have attached. If so, gently aspirate Plating Medium and replace it with 1 ml of Maintenance Medium. Cells can be maintained for up to 4 weeks. No changing of medium is necessary.

COMMENT: Because of necessity of transfection, cells can be used for experiment as early as 1DIV.

Transfecting the cells with SEP-containing DNA construct TIMING 1,5 h

CRITICAL This protocol was used to monitor GLT1-SEP in astrocytes in mature hippocampal culture but transfection can be done earlier depending on the biological question asked. I should be noted that transfection after 10-12 DIV, results usually in much lower efficiency.

24. At 7-9 days in vitro remove 0.5 ml of Maintenance Medium from each well for transfection and keep it until it is used in step 27 of the Procedure.
25. Prepare DNA-Lipofectamine 3000 complexes according to the manufacturer's instructions using plasmid DNA from Step 4 and incubate them at RT for 15 minutes.
CRITICAL STEP For most DNA constructs it is necessary to experimentally establish the amount of plasmid required for optimal expression.
26. Add dropwise 50 µl of DNA-Lipofectamine complexes to the cells in the remaining ~0.5 ml of Maintenance Medium. Gently rock the plate to mix.
27. Incubate cells with DNA-Lipofectamine for 45 min – 1h in the incubator.
28. Gently aspirate transfection mixture, and return 0.5 ml of conditioned medium kept from step 24 plus 0.5 ml of fresh Maintenance Medium.
CRITICAL STEP Avoid drying the cells. Work with one well at a time.
29. Incubate cells for at least 72h, so that there is enough time to for expression to reach the intracellular/membrane equilibrium for the protein. In our experiments we have waited

7-11 days after transfection in order for the culture reach sufficient maturity **when neuronal cultures develop fully functional synapses.**

CRITICAL STEP It is important to check if the expressed construct of the membrane protein (here GLUT1) in fusion with SEP is directed to the membrane, and ensure that the fusion tag does not affect the protein's function. Depending on the protein of interest this can be done by performing immunocytochemistry or by other means, for example electrophysiology, enzymatic assays, etc.

Preparation of the imaging setup TIMING 1h

30. Switch on two-photon imaging setup and femtosecond-pulse lasers, warm ES to 34°C and fill in the perfusion system.
31. Turn on perfusion system and switch on in-line heating, setting it to 34°C. Wait for the temperature to stabilize for at least 15 minutes.
32. If your system has two tuneable lasers, one should be set at 910 nm for SEP imaging and one at 690 nm for bleaching; when using a single laser, set its wavelength at the absorption maximum of the tag. Keep imaging laser output power as low as practical, ensuring it does not exceed 4 mW (measured under the objective), and bleaching laser power at 10-12 mW.

CRITICAL STEP The imaging laser power must be kept low to avoid photodamage, so it is important to measure laser output power under the objective. The same is important for the bleaching laser as most of the cell surface is bleached in the experiments.

CAUTION Exposure to laser light can cause significant damage to the eyes. A collimated laser beam should be fully enclosed throughout in the path from the laser source to the objective back aperture. At the wavelength of >910 nm the beam is invisible. If your setup has at any point an open beam path for operational reasons, wear protective eyewear and remove any jewellery from your hands.

33. Using a patch pipette puller, pull a puffing pipette with a tip diameter of ~10 µm and fill it with NH₄Cl-ES (you can add 100 µM Alexa Fluor 633 to visualize puffed solution). Mount the pipette in a puff pipette holder. Alternatively, a standard patch pipette holder with a removed platinum electrode can be used.
34. Switch on Pneumatic PicoPump, set the regulator on a N₂ cylinder to 4-5 Bar and the PicoPump output pressure to ~ 55 kPa. It might be necessary to adjust the output pressure depending on the length of the tubing leading from a PicoPump to the puff pipette and puff pipette opening, to ensure sufficient solution exchange.

Cell imaging TIMING < 1h per coverslip

35. With the help of tweezers, take a coverslip with transfected cells and place it in a chamber of the upright microscope setup.
36. Focus on the cell layer and select a transfected cell for imaging.

CRITICAL STEP Try to choose cells with average expression level of the transfected construct. Very high expression is often a sign of an unhealthy cell which will negatively affect the experiment.

?TROUBLESHOOTING

37. Move the puff pipette tip to the edge of the field of view using the micromanipulator (Fig. 3a).

CRITICAL STEP This is an example of a control experiment that aims to ~~confirm or correct the surface fraction estimate (of the tagged protein) obtained using the whole-cell FRAP protocol.~~ estimate the surface fraction of the tagged protein. Another, complementing control experiment is acidification of the extracellular medium to silence tagged molecules on the cell surface, as explained in Experimental Design and detailed previously ¹. Other control experiments could be relevant to the molecule of interest.

CRITICAL STEP The puff pipette should be raised ~ 100 μm above the cell so that the pressure from the pipette tip won't blow the cell from the coverslip. The correct position must be optimised by the experimenter and will vary according to the cell type and its size. We often include 100 μM Alexa Fluor 633 Hydrazide in the puffed buffer to visualize the puff in a separate imaging channel.

38. Start time-lapse recording of NH_4Cl -ES application to assess membrane vs. total GLT1-SEP expression (Fig. 3b). We typically use a 512x512 frame with pixel dwell time of 4 μs and 4x zoom. This results in a frame time of 1.644 s. In the imaging software set up a trigger to open a pressure valve of the Pneumatic PicoPump and start puffing. We usually switch the puff on after 10 frames for the duration of 10 frames (Fig. 3).

?TROUBLESHOOTING

39. Briefly examine the recorded image. The application of NH_4Cl -ES should be easily visible as an increase of cell fluorescence (Fig. 3b). After the puff, the fluorescence should return to the baseline level. Wait for at least 5 min before moving to the next step.

CRITICAL STEP If, after the puff, the fluorescence level does not return to baseline, the cell should be discarded as its intracellular compartments might have been permanently alkalinized. In general, there should be an at least 5 min break between pH manipulation and the start of the FRAP experiments. As described in Experimental Design, the NH_4Cl puffing experiments, which help establish the membrane fraction of the tagged protein (termed R , see Experimental Design) can be performed in a separate group of cultures.

40. At the start of the whole-cell FRAP experiments it is preferable to keep the same imaging conditions as for the puff experiment above. Use the laser-scanning microscope control software to select a circular region (ROI-PB) to be bleached using a "tornado mode" (Fig. 3d). We routinely use a circle of 398-pixel diameter, with 10 μs pixel dwell time, which results in bleaching the ROI-PB in just 2 s. The ROI-PB is usually selected so that a some of cell processes remain unbleached, to maintain a reference region for residual correction of photobleaching.

41. Initiate the bleaching sequence after 15-20 frames imaged in baseline conditions (bleaching with intense laser light will be readily detectable in recorded images) and continue to collect image frames until full recovery from photobleaching, as established empirically; in our case it was 200 frames, or 5-6 min (Fig. 3d). Monitor the cell for any unhealthy signs, such as shrinkage or swelling; some minor movements of cell processes are normal.

?TROUBLESHOOTING

42. Save and catalogue the stack of recorded time-lapse frame images for off-line analyses, including the metafiles containing all the ROI and timing data for the experiment.
43. Record 2-4 cells from the same coverslip. We advise keeping one coverslip under the microscope for < 1h in total. If additional drugs are used, like inhibitors or agonists, then only one cell per coverslip should be recorded because drug washout is rarely complete whereas every new recorded cell would require a control / reference recording session without drugs.
44. At the end of the imaging session dispose of the puff pipette, and rinse and dry the perfusion system.

PAUSE POINT Saved stacks of time-lapse frame images can be analysed at a later time.

Off-line data analysis TIMING ~20 min per cell

45. First, analyse images of NH₄Cl puffing to establish the cell-surface fraction of membrane protein-SEP. Upload the recorded image stack file to an appropriate analysis software, for instance Fiji (or other ImageJ versions)⁷⁴ which we use here. Draw manually an ROI around the cell using the 'polygon' or 'free-hand' selection tool and record the time course of mean fluorescence; the exact definition of cell boundaries is not required but the ROI should be entirely inside the visible cell morphology.
46. The NH₄Cl puff neutralizes the pH in exocytotic vesicles and thus allows visualization of the total expression of SEP-tagged proteins in the cell. Plot the mean fluorescence over time and verify that it reaches a plateau during NH₄Cl puffing (Fig. 3c). Normalise the basal fluorescence level F_{bas} (collected during 2-3 s before the puff) to the averaged fluorescence level during the puff F_{puff} (collected over 1-2 s during the plateau). Check that after the puff the fluorescence level returns to F_{bas} within 10-20 s; if not adjust your imaging settings (reduce laser power) to avoid photobleaching. The normalised fluorescence ratio F_{bas} / F_{puff} represents the membrane fraction of the SEP-tagged protein.
47. To analyse data from whole-cell FRAP experiments, first upload the corresponding image data metafile with ROIs to Fiji; note the exact position of the bleached area, or ROI-PB, referring to your imaging system recordings (Fig. 4a, red circle). Select manually 3-4 smaller, 5-10 μm wide ROIs (~40 pixels in diameter) inside the recorded bleached area ROI-IB (Fig. 4a, orange circles), and another ROI to monitor background fluorescence F_b , away from the transfected cell (Fig. 4a, blue ROI).

48. Based on the saved time-lapse image frame stacks, record the fluorescence time course $F_{ROI}(t)$ within each small ROI using the 'Stack / Plot Z-axis profile' menus in Fiji; for convenience, set $t=0$ at the end of the photobleaching sequence (the point of minimal fluorescence).
49. Based on the saved time-lapse image frame stacks, record the fluorescence time course $F_b(t)$ of the background (Fig. 4a, blue ROI), as described in Step 47.
50. In each ROI, use the recorded fluorescence time course $F_{ROI}(t)$ to subtract the background fluorescence $F_b(t)$: $F'_{ROI}(t) = F_{ROI}(t) - F_b(t)$. In most cases, $F_b(t)$ will be constant throughout and thus represented by a single value, F_b . In some cases, $F_b(t)$ may report relatively strong baseline photobleaching during normal, low-intensity imaging. If $F_b(t)$ drops by >10% over the time relative to the FRAP time, fit the $F_b(t)$ time course with the single-exponent function $F^*(t)$ using standard software (e.g., Origin OriginLab).
51. In each ROI, use the recorded fluorescence time course $F'_{ROI}(t)$ to determine the basal fluorescence level F_0 , by averaging $F'_{ROI}(t)$ values over a 20-30 s interval (15-20 frames) prior to the photobleaching phase. In the case of strong baseline photobleaching (see Step 49), subtract the best-fit function $y_b(t) = Ae^{-k_b t} - 1$ from the recorded fluorescence time course $F'_{ROI}(t)$ beforehand.
52. In each ROI, subtract the minimal fluorescence at the end of the photobleaching period $F_{ROI}(t=0)$ from $F'_{ROI}(t)$ and F_0 and normalise the fluorescence time course $F'_{ROI}(t)$ by the basal fluorescence F_0 so that

$$F(t) = \frac{F'_{ROI}(t) - F'_{ROI}(t=0)}{F_0 - F'_{ROI}(t=0)},$$

which represents the FRAP kinetics course for a given ROI (marked by dotted circles in Fig. 4b).

53. Store each FRAP data set (2-5 ROIs per cell) represented by an individual $F'_{ROI}(t)$ in a suitable X-Y format using a software application equipped with a procedure for non-linear function fitting, for instance, OriginPro (Origin Lab). Run the fitting procedure using the template function

$$y(x) = A(e^{-k_b x} - e^{-k_f x})$$

with the free parameters A , k_f , and k_b representing, respectively, the mobile fraction, the FRAP rate, and the photobleaching rate. Because these parameters are orthogonal, the algorithm is usually convergent, providing a reliable fit (red lines in Fig. 4b). If the baseline photobleaching trend $F^*(t)$ has been subtracted beforehand, the value of k_b will be negligibly small, which simplifies the fitting. Thus, the optimal strategy would be to subtract the function $y_b(t) = Ae^{-k_b t} - 1$ from each $F'_{ROI}(t)$ for individual ROI, to remove the residual photobleaching component: the latter could differ among ROIs and thus represent a poorly controlled contribution when averaging. The resulting FRAP data sets should contain no detectable residual photobleaching component (Fig. 4c).

?TROUBLESHOOTING

54. Calculate the average FRAP kinetics using the individual ROIs, either for individual cells (marked by dotted circles in Fig. 4d), or across the entire sample if the preparations and recording conditions were deemed fully consistent.
55. Fit the average data set with the FRAP kinetic function

$$y(t) = A(1 - e^{-k_I t}),$$

to constrain the two free parameters, A and k_I , that represent, respectively, the membrane fraction of the tagged protein and its intracellular fraction (Fig. 4d).

TIMING

- Steps 1-4, Preparing DNA construct of membrane protein fused with SEP: 2 weeks
- Steps 5-12, Preparing coverslips for cell culture, 2 days, 5h hands-on time (cleaning of coverslips ~1.5 h, baking and cooling ~3h, coating with poly-DL-Lysine ~10 min per multiwell plate, rinsing ~20 min per multiwell plate, coating with laminin ~ per multi-well plate)
- Steps 13-22, Preparing mixed hippocampal culture, 2-3h, 1 week growth and development
- Steps 23-28, Transfecting the cells with prepared SEP-containing DNA construct, 1.5 h
- Steps 29-33, Preparation of the imaging setup, ~1h
- Steps 34-44, Cell imaging, 45 min – 1h per cell
- Steps 45-55, Data analysis, 30-35 min per cell

Troubleshooting

Troubleshooting advice can be found in Table 1.

Table 1. Troubleshooting table.

Step	Problem	Possible reason	Solution
35	No transfected cell can be found	The transfection efficiency is too low	Optimize the incubation time of the cells with the DNA-Lipofectamine complexes and the amount of DNA used.
		There is a bubble under the objective	Lift the objective and wipe it with lens cleaning tissue.
37	Puff application of NH ₄ Cl-ES doesn't change the SEP fluorescence	Pipette is blocked by air bubble	Withdraw the pipette from the solution to avoid damaging the cell, and try to remove the bubble by applying higher pressure in the PicoPump. If this doesn't help, change the pipette.
		Pipette is blocked by debris/dust	Change the pipette and filter the NH ₄ Cl-ES solution through a 0.2 μm filter

40	Cell shrinks or swells after bleaching	laser power used during bleaching is too high	Discard the acquisition, decrease laser power and choose another cell. You should still be able to easily observe a decrease in the fluorescence level after bleaching.
		Expression of SEP fusion protein is too high	Discard the acquisition and chose a cell with an average expression level. If the problem is persistent, decrease the amount of DNA used during transfection of cells
		Poor condition of the cultured cells	Discard acquisition and chose cells from different coverslips. If the problem is persistent, choose cells from a different preparation. Properly clean coverslips before use.
52	Function fitting fails	Choice of initial parameters is out of range	In the software application, select initial values of the free parameters A , k_f , and k_b that provide a crude first approximation of the fitting curve
		The data are too noisy, fitting is non-convergent	Discard ROI data set

Anticipated results

The present protocol provides a general experimental approach to evaluate the recycling rate of membrane proteins of interest on the cell surface, on the time scale of seconds or slower, in live cell preparations. Once this basic result has been established it enables a researcher to ask fundamental questions regarding the molecular mechanisms underpinning or regulating the protein turnover. Such functional analyses include ligand application, cell or network stimulation, or testing the importance of protein domains or point mutations for protein recycling and /or membrane mobility. As a characteristic example, in the particular case of GLUT1, once we established its membrane turnover rate in basal conditions (Fig. 5a), we truncated the protein's intracellular domain, which was hypothesised to interact with other protein partners involved in protein recycling. The removal of GLUT1's C-terminus reduced its characteristic membrane reappearance time constant from ~ 22 s to ~ 14 s (Fig. 5b), thus suggesting that the C-terminus plays an important role in 'anchoring' the protein to its membrane location¹. What other molecular players take part in regulating this process remains an intriguing question, which could be addressed in detail using the present protocol.

Data Availability

The original experimental data are available as Source Data files in the supporting primary research article ¹.

Author contributions

PM suggested and implemented genetic designs, planned and carried out experiments, and analysed the results; DAR narrated the study, designed imaging methods, and performed theoretical data analyses; DAR and PM wrote the manuscript.

Competing interests

The authors declare no competing interests.

Acknowledgements

The study was supported by: Wellcome Trust (212251_Z_18_Z), MRC (MR/W019752/1), ERC (323113) and European Commission NEUROTWIN (857562) to DAR; National Science Centre Poland (2017/26/D/NZ3/01017) to PM.

References

1. Michaluk, P., Heller J. P. & Rusakov D. A. Rapid recycling of glutamate transporters on the astroglial surface. *Elife* **10**, 64714 (2021).
2. Zhang, J., Campbell R. E., Ting A. Y. & Tsien R. Y. Creating new fluorescent probes for cell biology. *Nat Rev Mol Cell Biol* **3**, 906-918 (2002).
3. Lippincott-Schwartz, J. & Patterson G. H. Development and use of fluorescent protein markers in living cells. *Science* **300**, 87-91 (2003).
4. Axelrod, D., Koppel D. E., Schlessinger J., Elson E. & Webb W. W. Mobility measurement by analysis of fluorescence photobleaching recovery kinetics. *Biophys J* **16**, 1055-1069 (1976).
5. Lippincott-Schwartz, J., Altan-Bonnet N. & Patterson G. H. Photobleaching and photoactivation: following protein dynamics in living cells. *Nat Cell Biol Suppl*, S7-14 (2003).
6. Lambert, N. A. Uncoupling diffusion and binding in FRAP experiments. *Nat Methods* **6**, 183; author reply 183-184 (2009).
7. Choquet, D. & Triller A. The role of receptor diffusion in the organization of the postsynaptic membrane. *Nat Rev Neurosci* **4**, 251-265 (2003).
8. Bannai, H., Levi S., Schweizer C., Dahan M. & Triller A. Imaging the lateral diffusion of membrane molecules with quantum dots. *Nat Protoc* **1**, 2628-2634 (2006).
9. Betzig, E., *et al.* Imaging intracellular fluorescent proteins at nanometer resolution. *Science* **313**, 1642-1645 (2006).
10. Rossier, O., *et al.* Integrins beta1 and beta3 exhibit distinct dynamic nanoscale organizations inside focal adhesions. *Nat Cell Biol* **14**, 1057-1067 (2012).
11. Manley, S., *et al.* High-density mapping of single-molecule trajectories with photoactivated localization microscopy. *Nat Methods* **5**, 155-157 (2008).
12. Sydor, A. M., Czymmek K. J., Puchner E. M. & Mennella V. Super-Resolution Microscopy: From Single Molecules to Supramolecular Assemblies. *Trends Cell Biol* **25**, 730-748 (2015).
13. Giannone, G., *et al.* Dynamic superresolution imaging of endogenous proteins on living cells at ultra-high density. *Biophys J* **99**, 1303-1310 (2010).
14. Carion, O., Mahler B., Pons T. & Dubertret B. Synthesis, encapsulation, purification and coupling of single quantum dots in phospholipid micelles for their use in cellular and in vivo imaging. *Nat Protoc* **2**, 2383-2390 (2007).
15. Livet, J., *et al.* Transgenic strategies for combinatorial expression of fluorescent proteins in the nervous system. *Nature* **450**, 56-62 (2007).
16. Barnes, S. A., *et al.* Convergence of Hippocampal Pathophysiology in Syngap^{+/-} and Fmr1^{-/y} Mice. *J Neurosci* **35**, 15073-15081 (2015).
17. Politi, A. Z., *et al.* Quantitative mapping of fluorescently tagged cellular proteins using FCS-calibrated four-dimensional imaging. *Nat Protoc* **13**, 1445-1464 (2018).

18. Heal, W. P., Wright M. H., Thinon E. & Tate E. W. Multifunctional protein labeling via enzymatic N-terminal tagging and elaboration by click chemistry. *Nat Protoc* **7**, 105-117 (2011).
19. Kamiyama, D., *et al.* Versatile protein tagging in cells with split fluorescent protein. *Nat Commun* **7**, 11046 (2016).
20. Miesenbock, G., De Angelis D. A. & Rothman J. E. Visualizing secretion and synaptic transmission with pH-sensitive green fluorescent proteins. *Nature* **394**, 192-195 (1998).
21. Sankaranarayanan, S., De Angelis D., Rothman J. E. & Ryan T. A. The use of pHluorins for optical measurements of presynaptic activity. *Biophys J* **79**, 2199-2208 (2000).
22. Sankaranarayanan, S. & Ryan T. A. Calcium accelerates endocytosis of vSNAREs at hippocampal synapses. *Nat Neurosci* **4**, 129-136 (2001).
23. Matz, J., Gilyan A., Kolar A., McCarvill T. & Krueger S. R. Rapid structural alterations of the active zone lead to sustained changes in neurotransmitter release. *Proc Natl Acad Sci U S A* **107**, 8836-8841 (2010).
24. Ashby, M. C., De La Rue S. A., Ralph G. S., Uney J., Collingridge G. L. & Henley J. M. Removal of AMPA receptors (AMPA receptors) from synapses is preceded by transient endocytosis of extrasynaptic AMPARs. *J Neurosci* **24**, 5172-5176 (2004).
25. Ashby, M. C., Maier S. R., Nishimune A. & Henley J. M. Lateral diffusion drives constitutive exchange of AMPA receptors at dendritic spines and is regulated by spine morphology. *J Neurosci* **26**, 7046-7055 (2006).
26. Tanaka, K., *et al.* Epilepsy and exacerbation of brain injury in mice lacking the glutamate transporter GLT-1. *Science* **276**, 1699-1702 (1997).
27. Danbolt, N. C. Glutamate uptake. *Progr Neurobiol* **65**, 1-105 (2001).
28. Lehre, K. P. & Danbolt N. C. The number of glutamate transporter subtype molecules at glutamatergic synapses: Chemical and stereological quantification in young adult rat brain. *J Neurosci* **18**, 8751-8757 (1998).
29. Diamond, J. S. & Jahr C. E. Transporters buffer synaptically released glutamate on a submillisecond time scale. *J Neurosci* **17**, 4672-4687 (1997).
30. Wadiche, J. I., Arriza J. L., Amara S. G. & Kavanaugh M. P. Kinetics of a human glutamate transporter. *Neuron* **14**, 1019-1027 (1995).
31. Lozovaya, N. A., Kopanitsa M. V., Boychuk Y. A. & Krishtal O. A. Enhancement of glutamate release uncovers spillover-mediated transmission by N-methyl-D-aspartate receptors in the rat hippocampus. *Neurosci* **91**, 1321-1330 (1999).
32. Scimemi, A., Fine A., Kullmann D. M. & Rusakov D. A. NR2B-containing receptors mediate cross talk among hippocampal synapses. *J Neurosci* **24**, 4767-4777 (2004).
33. Zheng, K., Scimemi A. & Rusakov D. A. Receptor actions of synaptically released glutamate: the role of transporters on the scale from nanometers to microns. *Biophys J* **95**, 4584-4596 (2008).
34. Henneberger, C., *et al.* LTP Induction Boosts Glutamate Spillover by Driving Withdrawal of Perisynaptic Astroglia. *Neuron* **108**, 919-936 e911 (2020).

35. Maragakis, N. J. & Rothstein J. D. Glutamate transporters: animal models to neurologic disease. *Neurobiol Dis* **15**, 461-473 (2004).
36. Fontana, A. C. Current approaches to enhance glutamate transporter function and expression. *J Neurochem* **134**, 982-1007 (2015).
37. Kruyer, A., Scofield M. D., Wood D., Reissner K. J. & Kalivas P. W. Heroin Cue-Evoked Astrocytic Structural Plasticity at Nucleus Accumbens Synapses Inhibits Heroin Seeking. *Biol Psychiat* **86**, 811-819 (2019).
38. Al Awabdh, S., *et al.* Neuronal activity mediated regulation of glutamate transporter GLT-1 surface diffusion in rat astrocytes in dissociated and slice cultures. *Glia* **64**, 1252-1264 (2016).
39. Murphy-Royal, C., *et al.* Surface diffusion of astrocytic glutamate transporters shapes synaptic transmission. *Nat Neurosci* **18**, 219-226 (2015).
40. Sylantsev, S. & Rusakov D. A. Sub-millisecond ligand probing of cell receptors with multiple solution exchange. *Nature Protocols* **8**, 1299-1306 (2013).
41. Shen, Y., Rosendale M., Campbell R. E. & Perrais D. pHuji, a pH-sensitive red fluorescent protein for imaging of exo- and endocytosis. *J Cell Biol* **207**, 419-432 (2014).
42. Liu, A. Y., *et al.* pHmScarlet is a pH-sensitive red fluorescent protein to monitor exocytosis docking and fusion steps. *Nat Commun* **12**, (2021).
43. Lazarenko, R. M., DelBove C. E., Strothman C. E. & Zhang Q. Ammonium chloride alters neuronal excitability and synaptic vesicle release. *Sci Rep-Uk* **7**, (2017).
44. Reits, E. A. J. & Neefjes J. J. From fixed to FRAP: measuring protein mobility and activity in living cells. *Nat Cell Biol* **3**, E145-E147 (2001).
45. Jensen, T. P., Zheng K., Tyurikova O., Reynolds J. P. & Rusakov D. A. Monitoring single-synapse glutamate release and presynaptic calcium concentration in organised brain tissue. *Cell Calcium* **64**, 102-108 (2017).
46. Jensen, T. P., Zheng K. Y., Cole N., Marvin J. S., Looger L. L. & Rusakov D. A. Multiplex imaging relates quantal glutamate release to presynaptic Ca²⁺ homeostasis at multiple synapses in situ. *Nature Communications* **10**, 1414 (2019).
47. Gabriel, L., Stevens Z. & Melikian H. Measuring plasma membrane protein endocytic rates by reversible biotinylation. *J Vis Exp*, (2009).
48. Turvy, D. N. & Blum J. S. Biotin labeling and quantitation of cell-surface proteins. *Curr Protoc Immunol* **Chapter 18**, Unit 18 17 (2001).
49. Holton, K. L., Loder M. K. & Melikian H. E. Nonclassical, distinct endocytic signals dictate constitutive and PKC-regulated neurotransmitter transporter internalization. *Nat Neurosci* **8**, 881-888 (2005).
50. Scott, D. B., Michailidis I., Mu Y., Logothetis D. & Ehlers M. D. Endocytosis and degradative sorting of NMDA receptors by conserved membrane-proximal signals. *J Neurosci* **24**, 7096-7109 (2004).

51. Rizzolio, S. & Tamagnone L. Antibody-Feeding Assay: A Method to Track the Internalization of Neuropilin-1 and Other Cell Surface Receptors. *Methods Mol Biol* **1493**, 311-319 (2017).
52. Chiu, A. M., Barse L., Hubalkova P. & Sanz-Clemente A. An Antibody Feeding Approach to Study Glutamate Receptor Trafficking in Dissociated Primary Hippocampal Cultures. *J Vis Exp*, (2019).
53. Kim, S., Bell K., Mousa S. A. & Varner J. A. Regulation of angiogenesis in vivo by ligation of integrin alpha5beta1 with the central cell-binding domain of fibronectin. *Am J Pathol* **156**, 1345-1362 (2000).
54. Zilberstein, A., Snider M. D., Porter M. & Lodish H. F. Mutants of vesicular stomatitis virus blocked at different stages in maturation of the viral glycoprotein. *Cell* **21**, 417-427 (1980).
55. Pepperkok, R., *et al.* Imaging platforms for measurement of membrane trafficking. *Methods Enzymol* **404**, 8-18 (2005).
56. Passafaro, M., Piech V. & Sheng M. Subunit-specific temporal and spatial patterns of AMPA receptor exocytosis in hippocampal neurons. *Nat Neurosci* **4**, 917-926 (2001).
57. Hein, L., Ishii K., Coughlin S. R. & Kobilka B. K. Intracellular targeting and trafficking of thrombin receptors. A novel mechanism for resensitization of a G protein-coupled receptor. *J Biol Chem* **269**, 27719-27726 (1994).
58. Hopp, T. P., *et al.* A Short Polypeptide Marker Sequence Useful for Recombinant Protein Identification and Purification. *Bio-Technol* **6**, 1204-1210 (1988).
59. Leake, M. C., Chandler J. H., Wadhams G. H., Bai F., Berry R. M. & Armitage J. P. Stoichiometry and turnover in single, functioning membrane protein complexes. *Nature* **443**, 355-358 (2006).
60. Willig, K. I., Rizzoli S. O., Westphal V., Jahn R. & Hell S. W. STED microscopy reveals that synaptotagmin remains clustered after synaptic vesicle exocytosis. *Nature* **440**, 935-939 (2006).
61. Luo, N., Yan A. & Yang Z. B. Measuring Exocytosis Rate Using Corrected Fluorescence Recovery After Photoconversion. *Traffic* **17**, 554-564 (2016).
62. Chen, X., Zaro J. L. & Shen W. C. Fusion protein linkers: property, design and functionality. *Adv Drug Deliv Rev* **65**, 1357-1369 (2013).
63. Beaudoin, G. M., 3rd, *et al.* Culturing pyramidal neurons from the early postnatal mouse hippocampus and cortex. *Nat Protoc* **7**, 1741-1754 (2012).
64. Kaech, S. & Banker G. Culturing hippocampal neurons. *Nat Protoc* **1**, 2406-2415 (2006).
65. Lein, P. J., Barnhart C. D. & Pessah I. N. Acute hippocampal slice preparation and hippocampal slice cultures. *Methods Mol Biol* **758**, 115-134 (2011).
66. Jiang, M. & Chen G. High Ca²⁺-phosphate transfection efficiency in low-density neuronal cultures. *Nat Protoc* **1**, 695-700 (2006).
67. Chen, C. C., *et al.* Patch-clamp technique to characterize ion channels in enlarged individual endolysosomes. *Nat Protoc* **12**, 1639-1658 (2017).

68. Rathje, M., *et al.* AMPA receptor pHluorin-GluA2 reports NMDA receptor-induced intracellular acidification in hippocampal neurons. *Proc Natl Acad Sci U S A* **110**, 14426-14431 (2013).
69. Savtchenko, L. P., *et al.* Disentangling astroglial physiology with a realistic cell model in silico. *Nature Communications* **9**, 3554 (2018).
70. Drobizhev, M., Makarov N. S., Tillo S. E., Hughes T. E. & Rebane A. Two-photon absorption properties of fluorescent proteins. *Nat Methods* **8**, 393-399 (2011).
71. Hafner, G., *et al.* Mapping Brain-Wide Afferent Inputs of Parvalbumin-Expressing GABAergic Neurons in Barrel Cortex Reveals Local and Long-Range Circuit Motifs. *Cell Rep* **28**, 3450-3461 e3458 (2019).
72. Valenti, M. T., *et al.* The effect of bisphosphonates on gene expression: GAPDH as a housekeeping or a new target gene? *BMC Cancer* **6**, 49 (2006).
73. Nifosi, R. & Luo Y. Predictions of novel two-photon absorption bands in fluorescent proteins. *J Phys Chem B* **111**, 14043-14050 (2007).
74. Rueden, C. T., *et al.* ImageJ2: ImageJ for the next generation of scientific image data. *Bmc Bioinformatics* **18**, 529 (2017).

FIGURE LEGEND

Figure 1. Assessing membrane protein turnover using the pH-sensitive SEP tag and whole-cell FRAP: first principles.

(a) Diagram showing the insertion of super-ecliptic pHluorin into the outer domain of the target protein (GLT1); fluorescent light depicted in green. (b) Diagram illustrating kinetic exchange between intracellular (dark) and membrane (fluorescing) fractions of GLT1-SEP; k_i and k_r are the kinetic rates of membrane protein insertion and removal, respectively. (c) Diagram illustrating the pH manipulation test used to reveal the membrane fraction of GLT1-SEP: in baseline conditions, only membrane-bound GLT-1 fluoresces (left) whereas at pH=5.5 all GLT1-SEP become non-fluorescent (middle); making the cell membrane temporarily proton-permeable with NH_4Cl makes all cellular GLT1-SEP fluoresce (right); light blue circle, cell nucleus. (d) The principle of whole-cell FRAP to reveal the membrane turnover rates for the target protein: in baseline conditions, only membrane-bound GLT1-SEP fluoresce (left); photobleaching dims GLT1-SEP across the bulk of cell morphology (middle; photobleaching of all molecules within the red ROI-PB as shown here can be instead partial), and analysing a FRAP time course within smaller ROIs (dark blue circles, middle and right) reveals protein turnover kinetics.

Figure 2. Analysing whole-cell FRAP kinetics.

(a) Typical whole-cell FRAP time course illustrating the characteristic phases of the fluorescence kinetics, as indicated; dots, characteristic fluorescence intensity data recorded in individual ROIs in each frame during time-lapse frame imaging. (b) Fitting the theoretical FRAP function (see '*Whole-cell FRAP: estimating protein turnover rate*') to the experimental FRAP kinetics data illustrated in (a); residual photobleaching during the brief baseline period is ignored; see the text for further detail and theoretical derivations.

Figure 3. A full sequence of experiments in one cell: an example.

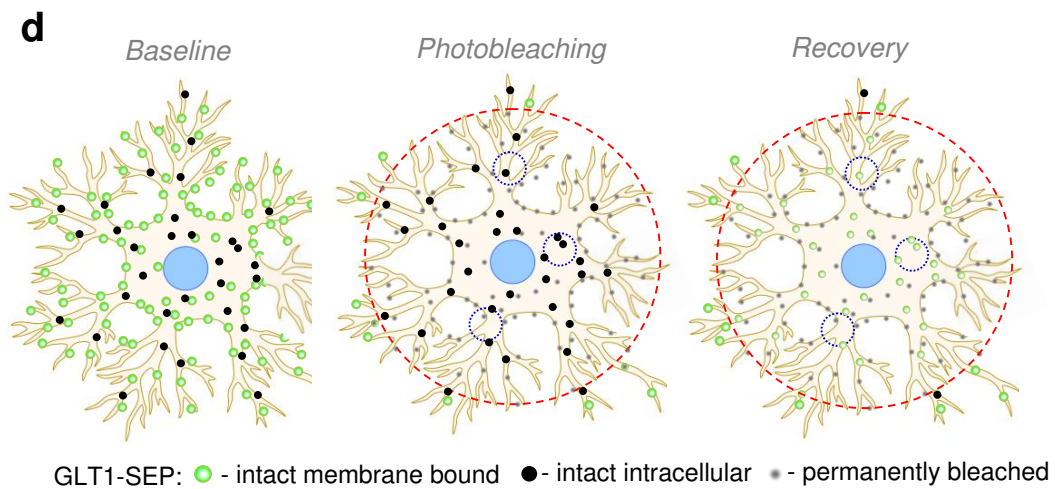
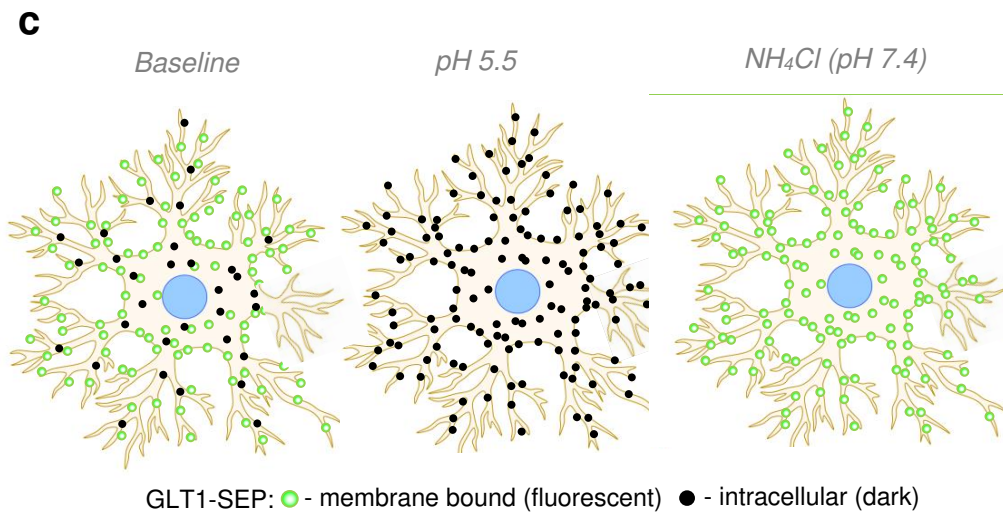
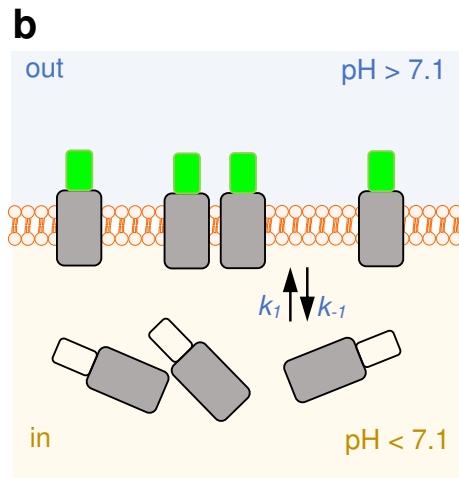
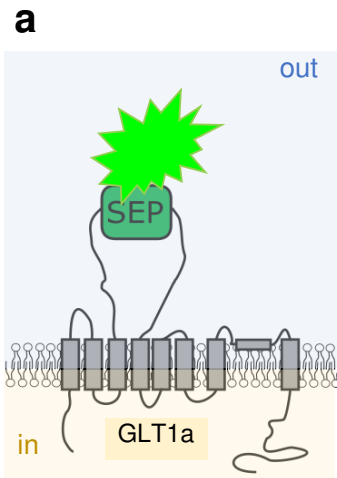
(a) A GLT1-SEP expressing astrocyte channel in mixed primary culture imaged in DIC + SEP fluorescence; the tip of a pressurised micropipette for local NH_4Cl application (with bright red-shifted traces Alexa 633 added for puff control) is seen. (b) Imaging snapshots showing the cell of interest before (left), during (middle), and after the NH_4Cl puff, in GLT1-SEP fluorescence channel (top), Alexa 633 channel (middle row, Alexa fluorescence reporting ejection spread), and merged channels (bottom). (c) Average fluorescence sampled over the extent of visible astrocyte morphology, during the experiment shown in (b), in the Alexa 633 and GLT1-SEP channels, normalised as indicated; grey shaded region, application of NH_4Cl . (d) Snapshots of the same cell undergoing a FRAP session at various time points, as indicated: in baseline conditions ($t=-25\text{s}$), during the photobleaching phase (at $t=0$), and during FRAP; dotted green circle, ROI-PB for whole-cell photobleaching; orange spiral, an illustration of the Tornado photobleaching scanning mode applied within the ROI-PB (green dotted circle).

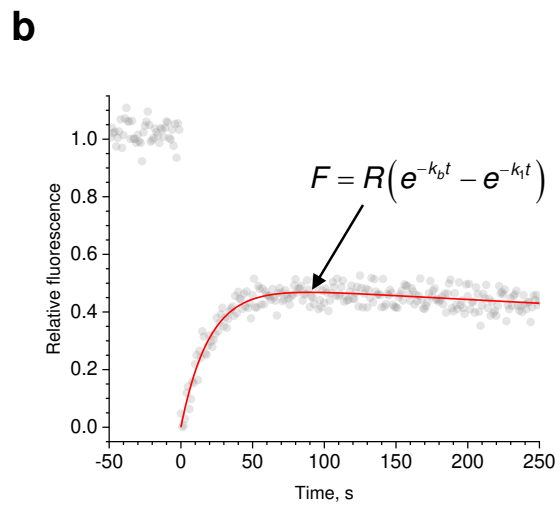
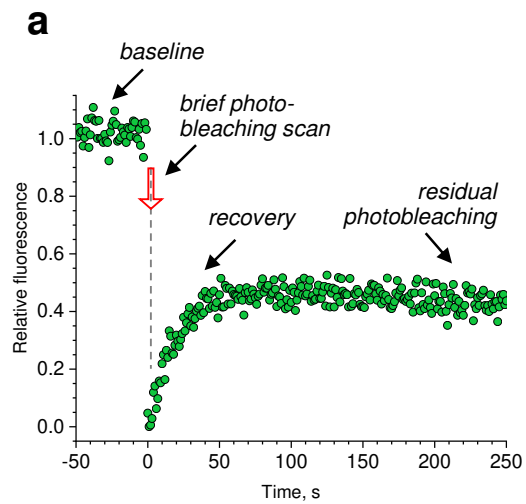
Figure 4. Analysing whole-cell FRAP data in one cell: an example.

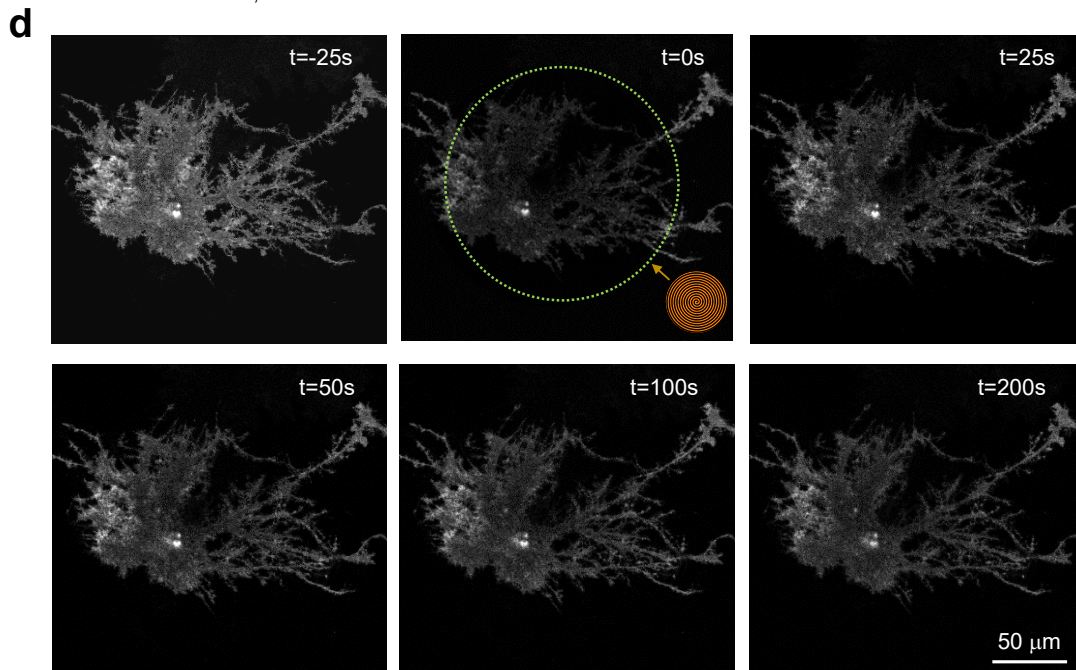
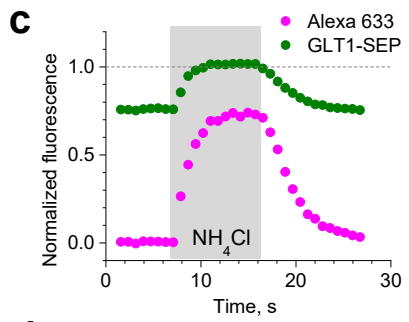
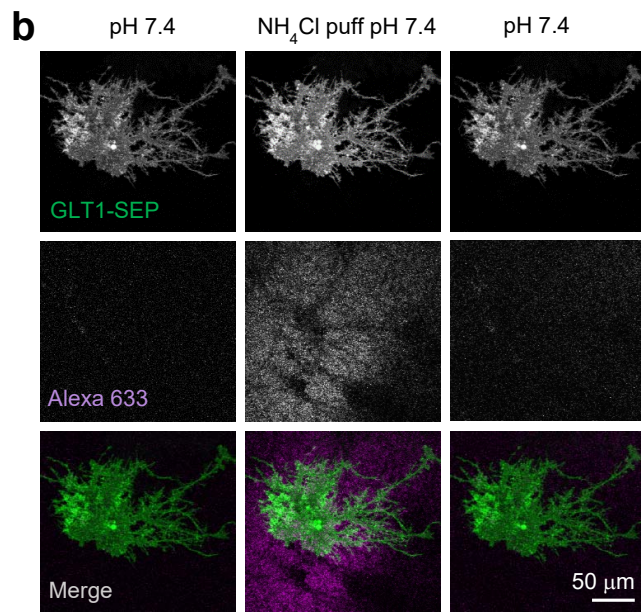
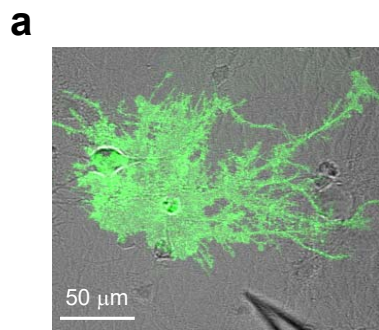
(a) An astrocyte shown with the selected ROI-PB (dotted red circle, photobleaching area), data collection ROI1-3 (yellow circles), and background ROI (dotted blue circle), as indicated. F_b , ROI used to measure background fluorescence. (b) Average fluorescence intensity data recorded in individual ROI1-3 as shown in (a) during the FRAP experiment, with background and the minimal ROI fluorescence value (at $t = 0$) subtracted, and the data normalised against the baseline fluorescence; solid lines, best-fit theoretical functions for the kinetics of GLT1-SEP FRAP (rate k_I , in s^{-1}) and photobleaching (rate k_b , in s^{-1}), using the fitting function $y(x) = A(e^{-k_b x} - e^{-k_I x})$, as illustrated in Fig. 2 and detailed in the text. (c) Experimental data as in (b) combined, with the photobleaching trend subtracted. (d) Experimental data from (c) averaged (dots; mean \pm SEM), with the best-fit theoretical FRAP kinetics (solid line), using the function $y(x) = A(1 - e^{-k_I x})$, which provides the estimated GLT1-SEP fraction (C_m / C_{tot}) and the protein membrane insertion rate (k_I , in s^{-1}), as indicated.

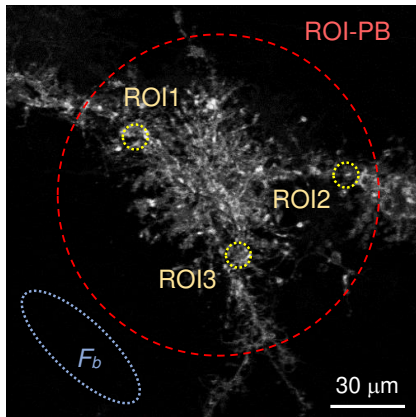
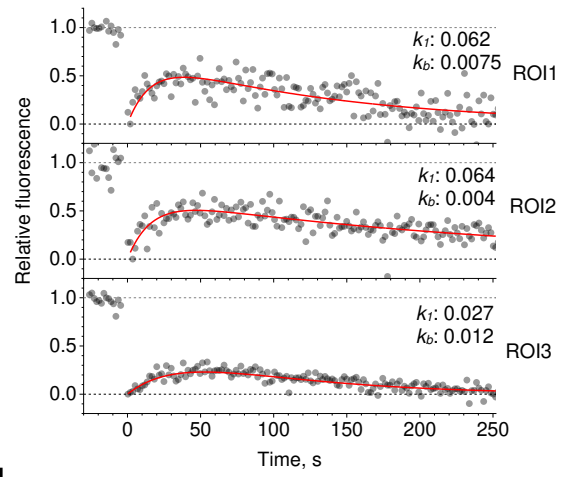
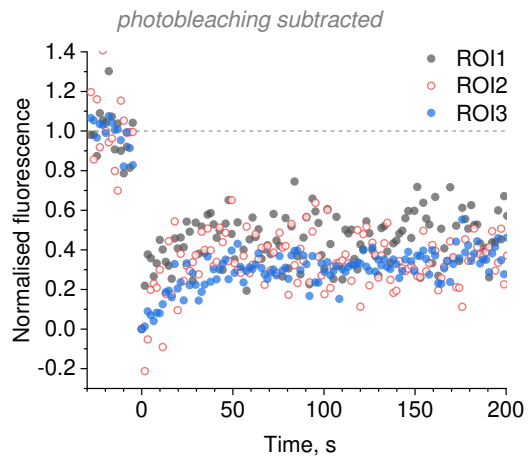
Figure 5. Anticipated results: an example.

(a) Whole-cell FRAP kinetics of GLT1-SEP across the experimental sample (dots, mean \pm SEM, $n = 27$ ROIs, 9 cells), with the best-fit theoretical function (solid line) providing the estimated intracellular fraction (C_{in}) and time constant of membrane insertion ($\tau_I = k_I^{-1}$), as indicated. (b) Whole-cell FRAP as in (a), but with the astrocytes expressing the GLT1 Δ C-SEP mutant with deleted C-terminus ($n = 25$ ROIs in $N = 8$ cells); other notations as in (a). Dataset from ¹.







a**b****c****d**